Active mixing by self-propelled Janus sponge Marangoni motors with self-maintaining surface tension gradients

Richard J Archer[1], Stephen J Ebbens[2], Yujin Kubodera[3], Muneyuki Matsuo[3,4]*, Shin-Ichiro M. Nomura[1]**

1) Molecular Robotics Laboratory, Department of Robotics, Graduate School of Engineering, Tohoku University, Sendai 980-8579, Japan.

2) Department of Chemical and Biological Engineering, University of Sheffield, Mappin Street, Sheffield S1 3JD, UK

3) Graduate School of Integrated Sciences for Life, Hiroshima University, 1-3-1 Kagamiyama, Higashi-Hiroshima, Hiroshima 739-8526, Japan

4) Graduate School of Arts and Sciences, The University of Tokyo

Correspondence; Shin-Ichiro M. Nomura (shinichiro.nomura.b5@tohoku.ac.jp), Richard J Archer (archer.richard.james.c8@tohoku.ac.jp).

Funding:

We acknowledge partial financial support from the JSPS KAKENHI grant

JP20H05701, JP20H05970, JP20H05968, JP20H00619, JP23K17485.

Keywords: Self-propulsion, Active-matter, Marangoni effect, Micromixers.

Abstract

Small scale Marangoni motors, which self-generate motion by inducing surface tension gradients on water interfaces through release of surface-active "fuels", have recently been proposed as self-powered mixing devices for low volume fluids. Such devices could lead to drastic rate improvements in processes reliant on diffusion limited reactions, without reliance on externally powered actuation, allowing for off-grid applications. Such devices however, often show self-limiting lifespans due to the rapid saturation of surface-active agents, resulting in a loss of motion far before depletion of their "fuel". A potential solution to this is the use surface-active agents which do not persist in their environment. Here we investigate menthyl acetate as a safe, inexpensive and convenient fuel for Marangoni motors. Menthyl acetate is a hydrophobic oil which reacts slowly with water to produce menthol, a high vapor pressure surface active agent. We demonstrate millimetre scale silicone sponge Marangoni motors, loaded with asymmetric "Janus" distributions of menthyl acetate show velocities and rotational speeds up to 30 mm s^{-1} and 500 RPM respectively, with their functional lifetimes scaling linearly with fuel volume. We show these devices are capable of enhanced mixing of solutions at orders of magnitude greater rates than diffusion alone.

1. Introduction.

Mixing of low volume fluids is an important requirement of many processes which rely on mass transport limited chemical reactions. Diffusion alone is a slow process which can impede the performance of medical diagnostic tools such as immunoassays, and mixing has

demonstrated potential to improve speed and sensitivity.[1–3] Typical mechanical mixing requires additional devices and a source of power to provide external actuation and agitation of fluid, for example the common use of orbital shakers during diagnostics. These requirements can limit such technologies to areas with established electrical infrastructures. Many emerging technologies, such as in point of care testing, would benefit greatly from being freed from the need for power sources. A potential solution to this problems would be small-scale, self-powered mixing devices which could be used "off-grid", broadening the practicality of rapid diagnostic devices in remote locations.[4–6] Interest in small scale self-powered devices has been gaining traction. Such self-powered devices typically generate forces by producing localized gradients, or releasing bubbles.[7–9] Here we investigate self-powered devices which use a simple chemical reaction to generate a localized surface tension gradient to induce motion for the purpose of fluid mixing. While many self-powered systems have been reported for self-generating motion,[10] one of the oldest and simplest is through establishing surface tension gradients.[11] Any chemical species which can sufficiently affect the surface tension of water is capable of producing mass transfer at fluid interfaces, known as the Marangoni effect.[12–14] Marangoni motors are objects which self-produce a surface tension imbalance across their body to drive their own motion.[15,16] Marangoni motors can carry their own "fuel" such as surfactants.[17] These systems however, only work until surface tension modification saturation is reached, after which the release of further "fuel", no longer induces a gradient and the motion irreversibly stops.[18] Various methods have been used to extend the life of Marangoni motors including slow release of surface active agents[19–21], post-release inactivation of surface active agents,[22,23] or using surface active agents without environmental permanence, such as volatile substances.[24]

A classic example is camphor crystals which have long been known to show long-acting spontaneous motion on the surface of water. Camphor, which has poor solubility in water (1.2

g L^{-1}), slowly dissolves into water and locally reduces the surface tension around the crystal producing motion.[11,25–28] Camphor, a volatile solid, is able to evaporate from the water, preventing saturation and maintaining its surface tension driven motion. Loading of camphor into desired devices however is difficult due to its high melting point (170 ^{o}C) and therefore often requires a solvent to manipulate and use.[29] While camphor is inherently a surface active agent, menthyl acetate is a hydrophobic oil which slowly hydrolyzes in the presence of water to produce acetic acid and the desired surface active agent, menthol (Figure 1a). The acetate hydrolysis acts as a rate limiting step and the production of menthol results in marked lowering effect on the surface tension of water due its ability to disrupt hydrogen bonding.[30,31] Like camphor, menthol is a volatile substance and so the surface tension lowering effect is non-permanent as it evaporates from the water interfaces (Figure 1b). A consequence of this is to overcome the saturation limit in previous devices and so increase the longevity of the motion due to the surface tension gradient being maintained. In contrast to camphor, menthyl acetate is a liquid at room temperature (melting point 23 °C) and therefore typically requires no further processing to use as 'fuel'. In this work we investigate the use of MA as a convenient and effective fuel for creation of Marangoni motors (Figure 1c). We show that MA based self-powered devices are capable of high velocities for extended periods of time and often demonstrate spinning motion. Finally, we demonstrate that the surface tension disruption in combination with the rapid motion of Marangoni motor generates a large fluid flow which can be used for efficient and rapid mixing of a solution far beyond passive diffusion (Figure 1d).

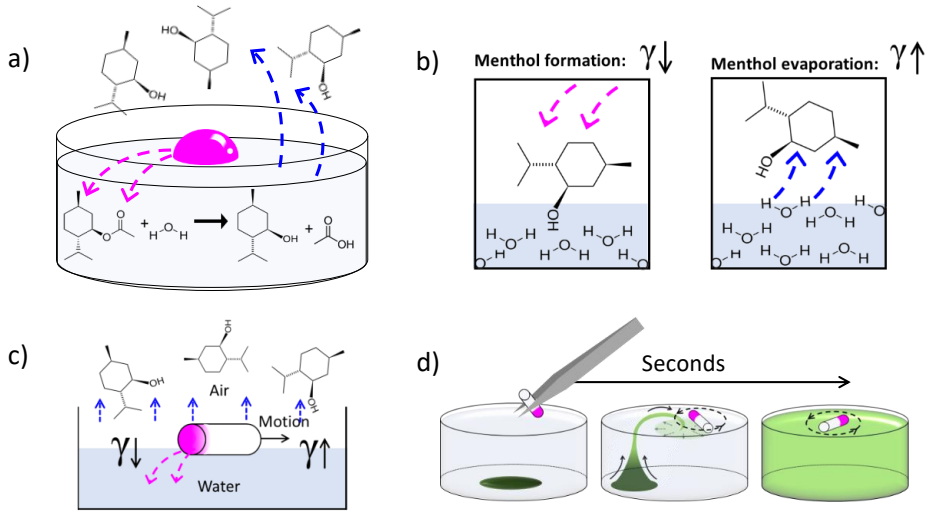

Figure 1. (a) Schematic showing menthyl acetate 'fuel' (pink) reacting with water in a body of water to form menthol (pink arrows) and acetic acid, the menthol then evaporates away (blue arrows). (b) Schematic to show menthol formed from the reaction at the interface of the water and lowering the surface tension (γ↓, left) followed by the recovery of the surface tension as menthol evaporates away (γ ↑, right). (c) Schematic to show an asymmetric distribution of menthyl acetate generating a surface tension gradient to drive motion of an object. (d) Schematic showing active motion of MA-sponge mixing a heterogenous concentrated solute (green) to homogenously dispersed solution.

2. Materials and Methods

Materials

Dimethyldimethoxysilane (DMDMS, 95%), methyltrimethoxysilane (MTMS, 98%) and sodium dodecyl sulfate (SDS) was purchased from Sigma-Aldrich. Urea (99%) was purchased from Nacalai Tesque Inc., Menthyl acetate (MA, 98%), cetyltrimethylammonium chloride (CTAC, 95%) were obtained from Tokyo Chemical Industry, Ltd., Colloidal solution (Polybead® Green Dyed Microbeads 1.06 µm diameter 2.6 wt%) was supplied by Polysciences, inc.

Sponge formation and shaping

Silicone sponges were prepared in a sol-gel process reported by Hayase et al.[32] Briefly, CTAC and urea were added to a solution of acetic acid and stirred until completely dissolved.

DMDMS and MTMS were then added to the CTAC/Urea solution and stirred for 30 minutes before heating to 80 ^{o}C overnight in a sealed container to form the siloxane gel. The final concentrations of the sol were acetic acid (5 mM) (urea 0.25 g/ml) (CTAC 0.05 g/ml) (MTMS 0.15 ml/ml) (DMDMS 0.1 ml/ml). The resulting gel was then thoroughly washed by cycles of water and ethanol to remove CTAC and urea. The sponge was finally dried from ethanol to give the porous hydrophobic silicone sponge (Figure 2a).

Rod shaped sponges were produced using a biopsy punch with 0.5 or 1.5 mm diameters to give cylindrical sponges with the desired width and finally cut to the desired length by a craft knife.

Marangoni motor formation

MA "fuel" was added by micropipette to one end face of the pre-cut sponge rod (Figure 2b). MA was readily absorbed by the sponge and formed a fuel gradient which correlated to the quantity of MA added. MA was used as supplied for motion analysis or dyed with Nile red to 0.1 wt% for visualization purposes.

Motion analysis

MA-sponges were placed on the surface of deionized-water filled petri dish (30 mm diameter containing 3 ml water) to begin the reaction and generate motion by surface tension gradients (Figure 2b). A smart phone video camera was placed at a set distance of 177 mm above the petri dish to record videos (30 or 60 Hz frame rate) for analysis. Video files were analyzed using custom image analysis routines developed using LabView software (National Instruments, UK) to quantitatively assess the stirrers motion. A pattern matching algorithm was used to determine the stirrers center of mass (COM) X, Y position and orientation for each frame in the video. A still frame containing a stirrer at a known orientation was used as the template for the pattern matching routine. The X, Y position and orientation data as a function of time were converted to instantaneous velocity (calculated as the COM displacement between

successive frames divided by the time gap between frames) , velocity decay (determined as a linear fit to instantaneous velocity v time plots), instantaneous rotational speed in revolutions per minute (RPM- (calculated from the change in orientation between successive frames divided by the time gap between frames) and rotational decay (again determined by a linear fit to rotation versus time data), the X, Y data was also used to generate trajectories for visualizing the devices COM motion in the figures shown below. (Figure SI 1a,b)

Surface tension measurement

Surface tension was measured using the Wilhelmy method. A tensiometer was made by placing a microbalance (Mettler Toledo, ME54) above the sample, a platinum wire (rod) was hung from the bottom sensor of the balance by string. The wire was adjusted to the meniscus of the water and slowly pulled out to measure the surface tension pull on the wire. All results are compared to deionized water and the relative force is assumed to be a linear correlation. To measure the surface tension over time the platinum rod was repeatedly dipped into and slowly withdrawn from the surface of the water. Data was recorded using B-LOGN data logger.

Mixing analysis

Mixing analysis was assessed by observing the dispersion of a concentrated deposit of green colored 1 µm latex colloids. The colloid suspension (1 µL, 2.6 wt% suspension) was added as a concentrated deposit by careful pipetting at the bottom of the petri dish. Videos were recorded to observe particle motion. ImageJ was used to record color intensity (intensity scale 0 to 1, black and white respectively) of still frames at 5 second intervals. The degree of mixing was determined as the inverse of the difference in color intensity between the darkest and brightest points of the solution (Excluding the sponge). A completely mixed solution would be defined as an observably homogeneous solution (100%) with no detectable differences in the color intensity of the solution.

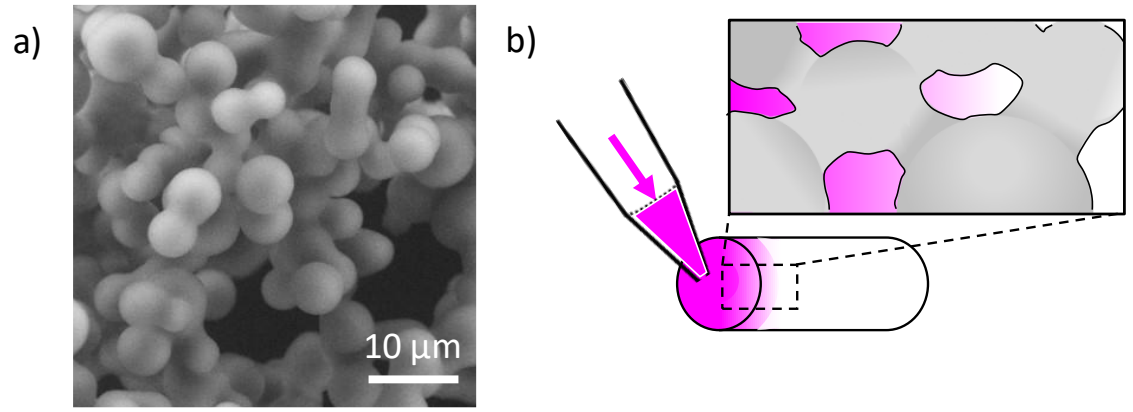

Figure 2. (a) SEM micrograph of the silicone sponge porous morphology (b) Schematic demonstrating the loading of menthyl acetate (red) into one end of a porous silicone material to create a "fuel" gradient within the device.

3. Results and Discussion

In all cases of the silicone sponges loaded with asymmetric distributions of MA "fuel", the sponge moves rapidly across an air/water interface. The motion of the sponge has a strong bias towards spinning motion or moving in tight circular paths (SM1). Their motion has a strong correlation to the MA fuel gradient. To assess the motion of MA-sponge systems as a function of the 'fuel' level, 1.5x4 mm sponges were used. MA was added at volumes of 0.1, 0.25, 1.0, 1.75 or 2.0 µL by micropipette to one end. Figure 3a, shows the MA fuel distribution after introduction of 0.1 to 2.0 µL of MA (dyed with Nile red for visualization, visualized here in pink), from one end of the sponge. Importantly, it can be easily seen that MA does not evenly distribute through the sponge structure, allowing for asymmetrical reactivity of the motor. Loading of 0.1 - 1.75 µL of MA resulted in a controllable and heterogenous distribution of 'fuel'. Loading of 2.0 µL of MA however, resulted in a saturated sponge without heterogeneity and therefore considered a symmetrically reactive system. Five videos per selected volume of MA were recorded and analyzed as described in the method section. Figure 3b-f show representative examples of x-y tracks of MA-sponge paths (red line) overlayed on the first image frame of the video from which the x-y plot was

obtained. With 0.1 µL of MA, the MA-sponge tended to take a very tight erratic path, as the volume of MA was increased the paths taken remained circular but became less erratic. The operational lifetime was directly proportional to the volume of MA fuel added to the sponge, indicating that no saturation of surface tension was achieved. The devices typically remained active for 3 to 30 minutes for 0.1 and 1.0 µL respectively (Figure 3g). Quantitative analysis of the motion revealed the average rotational speed for MA-sponges with 0.1 µL of MA was approximately 250 RPM (4 rotations per second), and the highest value reported was 500 RPM (8 rotations per second). Increasing the MA content in the sponge to even 0.25 µL resulted in a significant drop in rotational velocity to 60 RPM (1 rotation per second) and further decreases thereafter almost linearly to 50, 25 and 5 RPM for 1.0, 1.75 and 2.0 µL respectively (Figure 3h). The rotational velocity is seemingly highly sensitive to the MA distribution. Interestingly however, translational velocity increased from 20 to 30 mm s^{-1} as MA content was increased from 0.10 µL to 0.25 µL but linearly decreased to 15, 5 and 2 mm s^{-1} for 1.0, 1.75 and 2.0 µL respectively (Figure 3k). The initial increase in translational velocity followed by a steady decrease may indicate an interesting balance between MA volume and distribution. With higher MA loading, more reaction output would occur but localization of the fuel may affect the efficiency in the resulting motion (SM2).

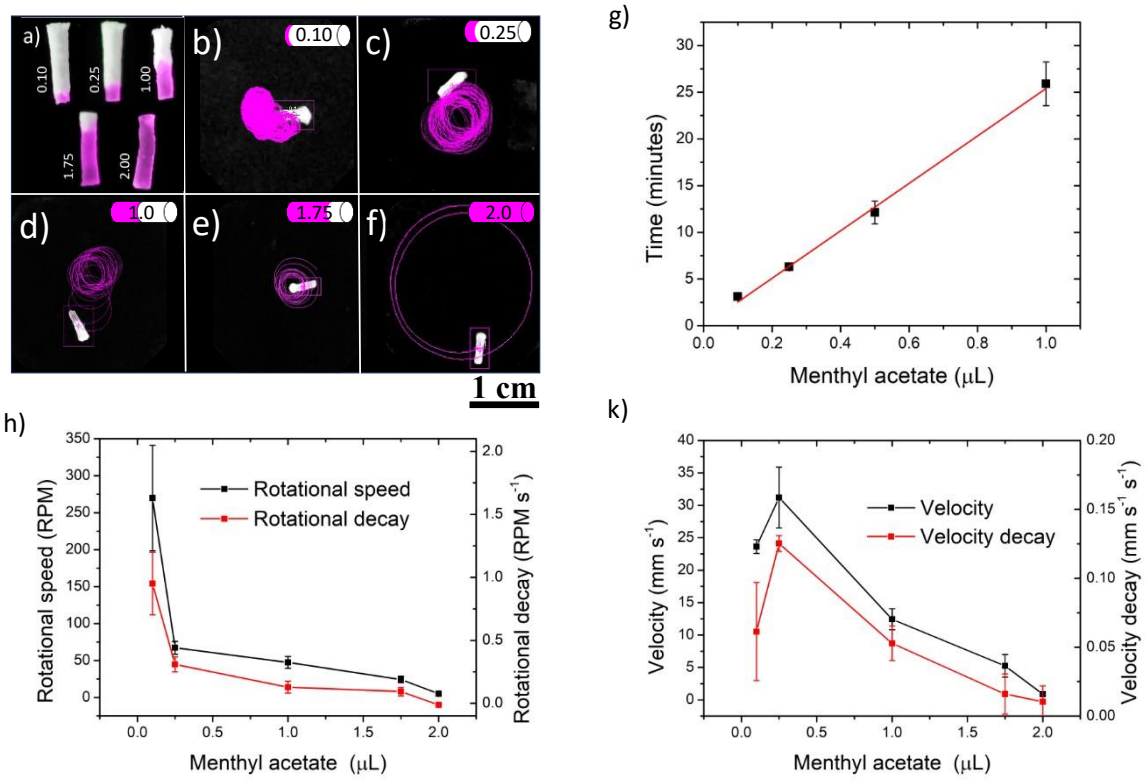

Figure 3. (a) Silicone sponges cut by biopsy punch to 4x1.5 mm and loaded with menthyl acetate (0.1, 0.25, 1.0, 1.75 and 2.0 µL) stained with Nile Red for visualization. (b-f) Singular frame image taken from 60 second movies overlayed with x,y plot of sponge center of mass from each video frame for menthyl acetate loading of 0.1, 0.25, 1.0, 1.75 and 2.0 µL respectively. (g) Measurement of effective motion lifetime by MA volume (h) Measurement of sponge Marangoni motor rotation as a function of menthyl acetate loading. (k) Measurement of sponge Marangoni motor linear velocity as a function of menthyl acetate loading.

The relatively long operational life of these Marongoni motors was suspected to be due to the surface tension recovery, similar to camphor boats[33]. It was thought that the surface tension would be lowered locally around the reactive sponge and return to normal at a certain distance away from the reactive site, thus maintaining a surface tension gradient for the duration of the reaction. However, attempts to measure the surface tension in relation to the distance and position of the MA-sponge did not reveal any measurable differences. This may be an

experimental limitation in sensitivity as well as difficulty in reliably measuring surface tension at solid interfaces due to curvature of the meniscus.[34]

The surface tension of the water in a petri dish when either MA or MA-sponges were added, both showed a rapid initial drop (Figure 4). This initial drop was followed by a plateau in surface tension which was maintained for as long as the MA continued to react. Once the MA was consumed, the surface tension gradually recovered to base value, indicating a complete depletion of menthol from the water. This is in stark contrast to surfactant powered Marangoni motors which inevitably establish a surface tension equilibrium which never recovers[20,22,35]. SDS was used here to show the surface tension for surfactant dosed solutions do not change on the time-scales considered for these devices.

Key differences between MA-only and MA-sponge systems was the total drop in surface tension and the duration of the plateau before recovery. With MA only, the surface tension dropped by 27% for approximately 100 seconds as opposed to the MA-sponge system which dropped by 20% for approximately 250 seconds. This would likely indicate a lower MA reaction rate in the MA-sponge system due to decreased direct water-MA contact. These results indicate that future designs of MA based Marangoni motors could consider the matrix material (Porosity/surface area) as a method of controlling the reaction rate and surface tension drop. We also note that the silicone sponge without MA (Sponge only) had no measurable effect on the surface tension of water.

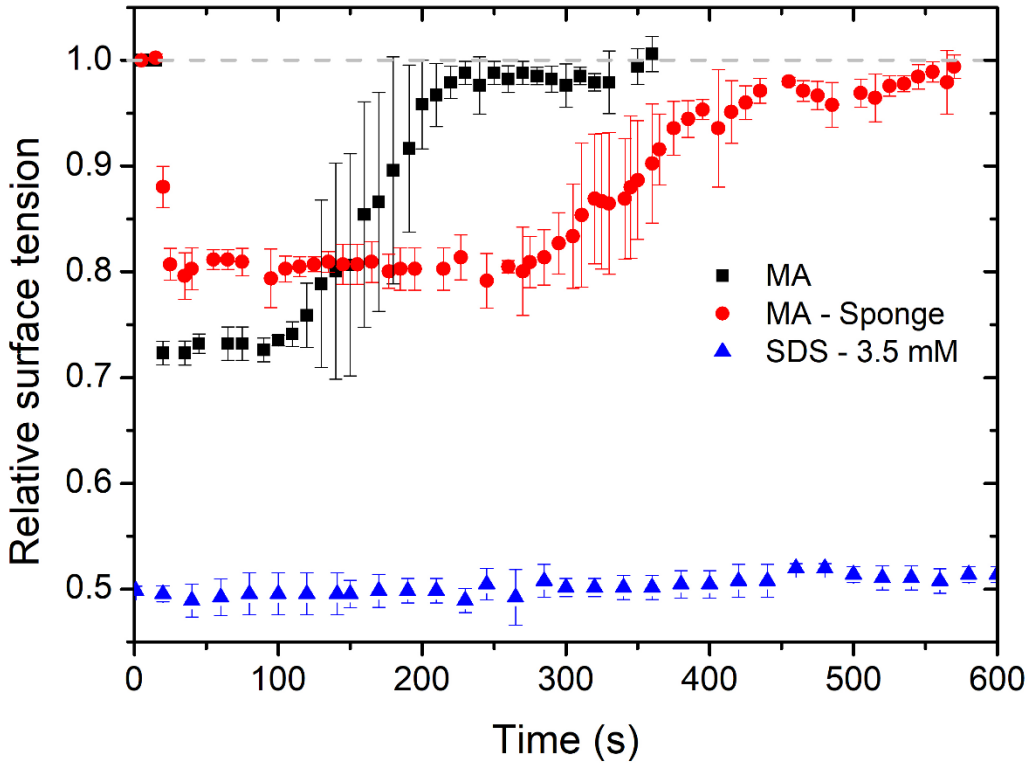

Figure 4. Surface tension measurements of deionized water with added menthyl acetate (0.2 µL MA), menthyl acetate loaded into the sponge (0.2 µL MA – 1.5x4 mm sponge) or the surfactant sodium dodecyl sulfate (SDS, final concentration 3.5 mM). All measurements reported are relative to the initial surface tension of the deionized water before any addition as indicated by the gray dashed line.

The evaporation of the menthol product is thought to be crucial to the surface tension recovery and consequently the continued motion of the Marangoni motors. To demonstrate this, a MA-sponge system (1.5x4 mm, MA µL) was added to a petri dish with water (30 mm, 3 ml) with the lid on (open) or off (covered) to control menthol evaporation rates (Figure 5a). In continuous experiments the lid would be off at the start followed by covering and opening, repeated twice to demonstrate reversibility. Initial translational velocity of the MA-sponge was

recorded at approximately 11 mm s^{-1}, in line with previous experiments. After 60 seconds, the lid was placed on (Cover 1) and the translational velocity quickly dropped to below 5 mm s^{-1} within seconds and finally came to a complete stop within 20 seconds of covering the dish (Figure 5b). After 120 seconds, the lid was removed again (Open 1) and motility was restored within seconds. Interestingly, after reopening, an initial velocity of approximately 17 mm s^{-1} was recorded, significantly higher than the starting velocity. Over the 60 second observation period the velocity of "Open 1" linearly declined towards the "Start" velocity. One explanation for this initial spike in velocity is caused by the prior menthol saturation of the system when covered in "Closed 1". Menthol saturation of the system would likely cause a decrease in the water surface tension below that from MA-sponge in an open system, as already seen between the MA-sponge and MA-only, Figure 4. The "Open 1" state would then establish a larger initial surface tension gradient as the saturated menthol quickly evaporates out of the system, causing the increased velocity observed. After the saturation dissipates, the initial balance between the reaction and evaporation would be re-established as reflected by the return of similar velocity rates. The covering and opening of the petri dish was repeated to show the reversibility of this effect ("Cover 2" and "Open 2" sequentially). "Cover 2" showed the same effect as "Cover 1" with a rapid loss of motion within seconds. "Open 3" however, showed a similar but diminished effect as "Open 2" with a lower initial velocity of 13 mm s^{-1}, followed by a linear decrease in velocity to 10 mm s^{-1}. The same menthol saturation effect is likely occurring but due to MA depletion over time this effect becomes weaker as the fuel is consumed and less menthol is produced.

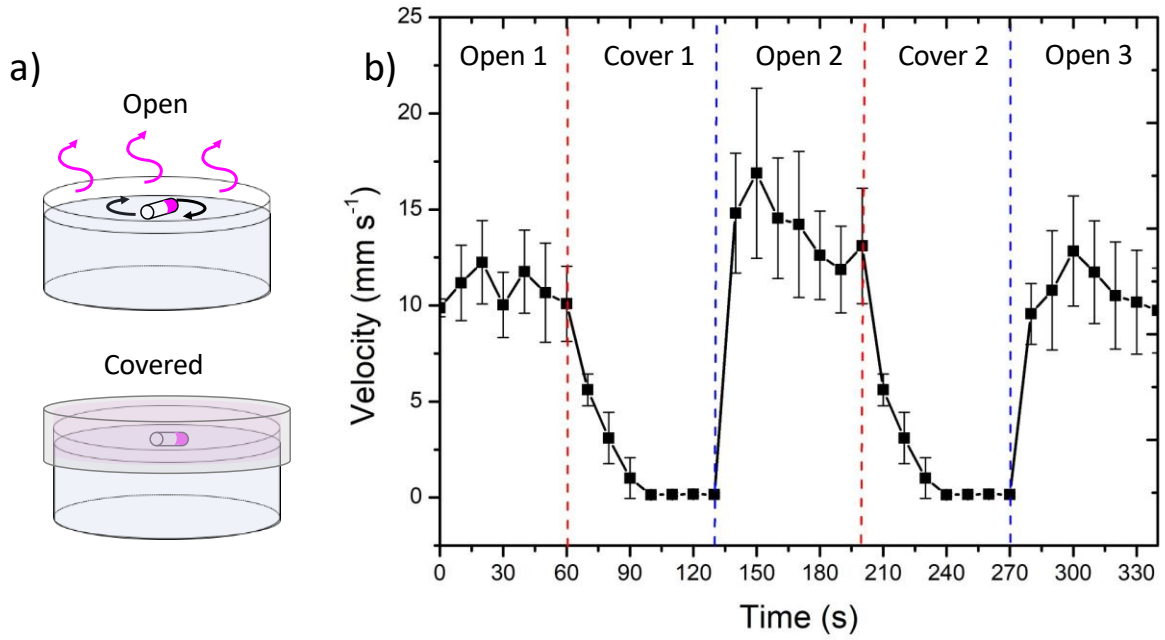

Figure 5. (a) Schematic illustration of Janus Marangoni motors spinning when the container is open and menthol (red) can be released (top) or static when the container is covered creating a menthol saturated environment (bottom). (b) Velocity measurements of Marangoni motors through two repeats of covering (red) and opening (blue) of the container over 300 seconds.

Finally, the ability of micro-stirring devices to agitate the solution was assessed by observing their effect on a small, localized concentration of colloidal particles acting as tracers. latex beads at 1 µm diameter were carefully pipetted at the bottom of a volume of water. The Stokes-Einstein equation gives the diffusion of 1 µm latex colloids as 4.91×10^{-9} cm^2 s^{-1}, therefore particle diffusion by Brownian motion is not considered significant over the experimental time frame (60 seconds). Figure 6a shows representative images of the particle dispersion after 0, 4, 8 and 12 seconds, and Figure 6b gives quantified values of the inverse percentage pixel intensity differences in the solution. Without MA (No MA), with MA droplets (0.1 µL) pipetted directly onto the water surface (MA-only) or MA (0.1 µL) loaded sponges (MA-sponge). In the absence of MA, the concentrated drop of latex beads did not significantly disperse over the duration of observation (SM3). A widening of the colloid rich droplet diameter is noticed. With

the direct addition of 0.1 µL MA onto the surface of water (MA-only), it was observed that MA droplets could move quickly and randomly on the surface of water (SM4). Very little net displacement of MA droplets is seen over time due to rapid changes in direction. MA breaking the surface tension and motion of the droplets caused some agitation of the solution, the latex bead solution was pulled towards the surface of the water creating a vertical column of high concentration. Introduction of MA infused silicone sponges (MA-Sponges) caused a rapid and significant agitation of the water volume (SM5). In the first few seconds the colloidal rich suspension was pulled to the surface of the water, more specifically, the leading end of the trail seemingly moved towards the MA-sponge, where the surface tension would likely be lowest. As the sponge turned, the colloidal trail would bend to follow. Subsequently, the colloidal concentration was rapidly dispersed with most cases taking under 20 seconds for a visually complete dispersion.

In all samples the initial pixel intensity difference was approximately 60% (average background and colloidal concentration pixel intensity was 0.072 ± 0.013, and 0.66 ± 0.01 respectively), giving a designated solution homogeneity of 40%. Without any interference (No MA) solution homogeneity increases to 50% over 60 seconds. This small increase in homogeneity correlates with the observed gradual widening of the colloidal suspension and indicates a decrease in concentration through passive environmental effects such as gravity and surface vibrations through the benchtop. With the addition of 0.1 µL of MA (MA-only), a surprising increase in the pixel intensity difference is observed in the first 10 seconds resulting in a decrease in the solution homogeneity to 20%, with a small increase to 30% and a plateau thereafter. This decrease in homogeneity is likely caused by the observed pull of the colloidal suspension vertically, combined with the limitation of 2D top-down analysis, creating an appearance on concentrating effect. The measured pixel intensity would be a sum of the colloidal spread through the z-axis. Regardless of this limitation we consider that the MA-only

droplets failed to cause a practical dispersion of the latex beads as a high concentration region of colloids remained, even after long periods of time (over ten minutes). With MA-sponge systems the solution homogeneity sharply decreases in the first 5 seconds to 20%, again due to the initial vertical pull of the colloidal solution to the surface creating higher pixel intensity by top-down view. However, in the case of MA-sponge Marangoni motor, the solution homogeneity quickly increases from 5 to 20 seconds to over 95% as the colloids are dispersed through the solution and homogeneity is achieved. We note that 100% homogeneity is never achieved in this analysis method due to noise in the image causing variation in pixel intensity.

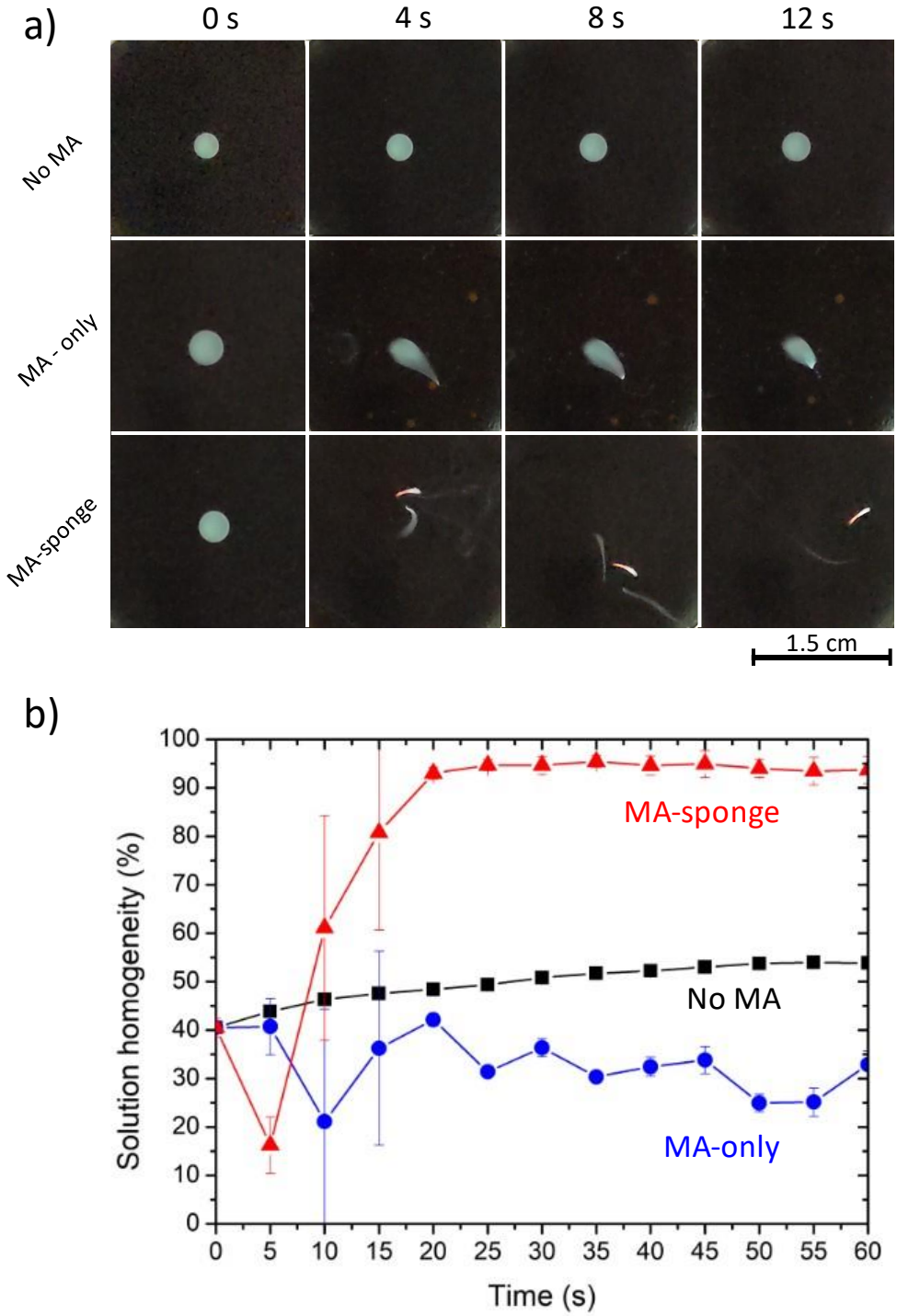

Figure 6. Dispersion of colloidal sediment (1 µL of 2.6 wt%) in a 3 cm petri dish with either no additives (No MA), 0.1 uL of menthyl acetate(MA-only) or 0.1 µL menthyl acetate loaded into 2 x 0.5 mm sponge (MA-sponge). (a) Still frames taken from video at 0 (before any addition), and 4, 8 and 12 seconds after addition of either MA or MA-sponge. (b) quantitative assessment of homogeneity by pixel intensity variation over 60 seconds, solution homogeneity is defined as the inverse of the pixel intensity difference.

As the rapid motion of the sponge seemed critical to the efficient mixing of the solution, an assessment of the motion as a function of the MA content was undertaken. The MA 'fuel' level was an inseparable function of both the volume of methyl-acetate and the length of the reactive gradient in the sponge. Both conditions must therefore be considered as contributing factors to their motion.

4. Conclusions

In summary, we have shown here a simple method to produce simple, low cost, millimeter scale chemical powered Janus motors which can be used to homogenize small aqueous volumes without need for external actuation. The Janus motors are shown to completely disperse a colloidal suspension within 20 seconds, far exceeding passive diffusion. These Janus motors could move at speeds of up to 35 mm s^{-1} and rotate at up to a peak of 500 RPM and averaging 350 RPM depending on their "fuel" gradient. The mechanism of motion is based on Marangoni flow caused by the production of surface tension lowering menthol from menthyl acetate reaction with water. Due to the volatility of menthol, the surface tension also recovers over time as it evaporates away. The effect of simultaneous formation and loss of menthol ensures the solution doesn't saturate and a surface tension gradient is maintained, greatly extending the lifespan when compared to surfactant driven Marangoni effects. Menthyl acetate by itself can agitate volumes of water but lacks sufficient effect to efficiently mix solutions. By introducing menthyl acetate into one side of a porous hydrophobic porous matrix, a simple Janus Marangoni motor can be produced. Generated motion for millimeter size Janus Marangoni motors can last from several up to tens of minutes for even microliter volumes (0.1-1.75 µL) of menthyl acetate. These Janus motors do not require any special equipment to make and are

completely re-usable, requiring only dabbing additional liquid fuel on to one end of the device. As the "fuel" is consumed and the volatile products evaporate away, this technique does not permanently alter the target solution, making this a potentially suitable method for analytical. Due to their ability to mix small volumes of liquids as well as their low cost, reusability, and their ability to work without external actuation, we believe these devices may be of interest in off-grid applications for assay mixing.

(1) Moghadam, B. Y.; Connelly, K. T.; Posner, J. D. Two Orders of Magnitude Improvement in Detection Limit of Lateral Flow Assays Using Isotachophoresis. *Anal. Chem.* **2015**, *87* (2), 1009–1017.

(2) Kusnezow, W.; Syagailo, Y. V.; Rüffer, S.; Klenin, K.; Sebald, W.; Hoheisel, J. D.; Gauer, C.; Goychuk, I. Kinetics of Antigen Binding to Antibody Microspots: Strong Limitation by Mass Transport to the Surface. *PROTEOMICS* **2006**, *6* (3).

(3) Hu, Q.; Ren, Y.; Liu, W.; Tao, Y.; Jiang, H. Simulation Analysis of Improving Microfluidic Heterogeneous Immunoassay Using Induced Charge Electroosmosis on a Floating Gate. *Micromachines* **2017**, *8* (7), 212.

(4) Choi, S. Powering Point-of-Care Diagnostic Devices. *Biotechnol. Adv.* **2016**, *34* (3), 321–330.

(5) Point-of-Care Technologies for Health Care. *IEEE Trans. Biomed. Eng.* **2011**, *58* (3), 732–735.

(6) Mitra, P.; Sharma, P. POCT in Developing Countries. *EJIFCC* **2021**, *32* (2), 195–199.

(7) Zhang, Y.; Gregory, D. A.; Zhang, Y.; Smith, P. J.; Ebbens, S. J.; Zhao, X. Reactive Inkjet Printing of Functional Silk Stirrers for Enhanced Mixing and Sensing. *Small* **2019**, *15* (1), 1804213.

(8) Ismagilov, R. F.; Schwartz, A.; Bowden, N.; Whitesides, G. M. Autonomous Movement and Self-Assembly. *Angew. Chem. Int. Ed.* **2002**, *41* (4), 652–654.

(9) Soler, L.; Magdanz, V.; Fomin, V. M.; Sanchez, S.; Schmidt, O. G. Self-Propelled Micromotors for Cleaning Polluted Water. *ACS Nano* **2013**, *7* (11), 9611–9620.

(10) Ebbens, S. J. Active Colloids: Progress and Challenges towards Realising Autonomous Applications. *Curr. Opin. Colloid Interface Sci.* **2016**, *21*, 14–23.

(11) Kitahata, H.; Hiromatsu, S.; Doi, Y.; Nakata, S.; Islam, M. R. Self-Motion of a Camphor Disk Coupled with Convection. *Phys. Chem. Chem. Phys.* **2004**, *6* (9), 2409–2414.

(12) Scriven, L. E.; Sternling, C. V. The Marangoni Effects. *Nature* **1960**, *187* (4733), 186–188.

(13) Kwak, B.; Choi, S.; Maeng, J.; Bae, J. Marangoni Effect Inspired Robotic Self-Propulsion over a Water Surface Using a Flow-Imbibition-Powered Microfluidic Pump. *Sci. Rep.* **2021**, *11* (1), 17469.

(14) Park, J.; Ryu, J.; Sung, H. J.; Kim, H. Control of Solutal Marangoni-Driven Vortical Flows and Enhancement of Mixing Efficiency. *J. Colloid Interface Sci.* **2020**, *561*, 408–415.

(15) Lauga, E.; Davis, A. M. J. Viscous Marangoni Propulsion. *J. Fluid Mech.* **2012**, *705*, 120–133.

(16) Renney, C.; Brewer, A.; Mooibroek, T. J. Easy Demonstration of the Marangoni Effect by Prolonged and Directional Motion: “Soap Boat 2.0.” *J. Chem. Educ.* **2013**, *90* (10), 1353–1357.

(17) Choi, Y.; Park, C.; Lee, A. C.; Bae, J.; Kim, H.; Choi, H.; Song, S. woo; Jeong, Y.; Choi, J.; Lee, H.; Kwon, S.; Park, W. Photopatterned Microswimmers with Programmable Motion without External Stimuli. *Nat. Commun.* **2021**, *12* (1), 4724.

(18) Kumar, P.; Zhang, Y.; Ebbens, S. J.; Zhao, X. 3D Inkjet Printed Self-Propelled Motors for Micro-Stirring. *J. Colloid Interface Sci.* **2022**, *623*, 96–108.

(19) Furukawa, K.; Teshima, T.; Ueno, Y. Self-Propelled Ion Gel at Air-Water Interface. *Sci. Rep.* **2017**, *7* (1), 9323.

(20) Ikezoe, Y.; Washino, G.; Uemura, T.; Kitagawa, S.; Matsui, H. Autonomous Motors of a Metal–Organic Framework Powered by Reorganization of Self-Assembled Peptides at Interfaces. *Nat. Mater.* **2012**, *11* (12), 1081–1085.

(21) Osada, Y.; Gong, J.; Uchida, M.; Isogai, N. I. N. Spontaneous Motion of Amphoteric Polymer Gels on Water. *Jpn. J. Appl. Phys.* **1995**, *34* (4B), L511.

(22) *Tackling the Short-Lived Marangoni Motion Using a Supramolecular Strategy*.

(23) Nomura, S. M.; Shimizu, R.; Archer, R. J.; Hayase, G.; Toyota, T.; Mayne, R.; Adamatzky, A. Spontaneous and Driven Growth of Multicellular Lipid Compartments to Millimeter Size from Porous Polymer Structures. *ChemSystemsChem* **2022**, *4* (5), e202200006.

(24) Jin, H.; Marmur, A.; Ikkala, O.; Ras, R. H. A. Vapour-Driven Marangoni Propulsion: Continuous, Prolonged and Tunable Motion. *Chem. Sci.* **2012**, *3* (8), 2526–2529.

(25) Nakata, S.; Iguchi, Y.; Ose, S.; Kuboyama, M.; Ishii, T.; Yoshikawa, K. Self-Rotation of a Camphor Scraping on Water: New Insight into the Old Problem. *Langmuir* **1997**, *13* (16), 4454–4458.

(26) Hayashima, Y.; Nagayama, M.; Nakata, S. A Camphor Grain Oscillates While Breaking Symmetry. *J. Phys. Chem. B* **2001**, *105* (22), 5353–5357.

(27) Karasawa, Y.; Oshima, S.; Nomoto, T.; Toyota, T.; Fujinami, M. Simultaneous Measurement of Surface Tension and Its Gradient around Moving Camphor Boat on Water Surface. *Chem. Lett.* **2014**, *43* (7), 1002–1004.

(28) Nakata, S.; Doi, Y.; Kitahata, H. Synchronized Sailing of Two Camphor Boats in Polygonal Chambers. *J. Phys. Chem. B* **2005**, *109* (5), 1798–1802.

(29) Li, X.; Mou, F.; Guo, J.; Deng, Z.; Chen, C.; Xu, L.; Luo, M.; Guan, J. Hydrophobic Janus Foam Motors: Self-Propulsion and On-The-Fly Oil Absorption. *Micromachines* **2018**, *9* (1), 23.

(30) Lewandowski, A.; Szymczyk, K. Adsorption of Monoterpene Alcohols at the Water–Air Interface. *Adsorption* **2019**, *25* (3), 301–308.

(31) Nunes, R. J.; Saramago, B.; Marrucho, I. M. Surface Tension of Dl-Menthol:Octanoic Acid Eutectic Mixtures. *J. Chem. Eng. Data* **2019**, *64* (11), 4915–4923.

(32) Hayase, G.; Nomura, S. M. Large-Scale Preparation of Giant Vesicles by Squeezing a Lipid-Coated Marshmallow-like Silicone Gel in a Buffer. *Langmuir* **2018**, *34* (37), 11021–11026.

(33) Burton, L. J.; Cheng, N.; Bush, J. W. M. The Cocktail Boat. *Integr. Comp. Biol.* **2014**, *54* (6), 969–973.

(34) Nomoto, T.; Marumo, M.; Chiari, L.; Toyota, T.; Fujinami, M. Time-Resolved Measurements of Interfacial Tension and Flow Speed of the Inclined Water Surface around a Self-Propelled Camphor Boat by the Quasi-Elastic Laser Scattering Method. *J. Phys. Chem. B* **2023**, *127* (12), 2863–2871.

(35) Toyota, T.; Maru, N.; Hanczyc, M. M.; Ikegami, T.; Sugawara, T. Self-Propelled Oil Droplets Consuming “Fuel” Surfactant. *J. Am. Chem. Soc.* **2009**, *131* (14), 5012–5013.